Inclusive charged-pion electroproduction*

C. J. Bebek, C. N. Brown,† M. S. Herzlinger,‡ S. D. Holmes,§ C. A. Lichtenstein,‖ F. M. Pipkin, S. W. Raither, and L. K. Sisterson¶

High Energy Physics Laboratory, Harvard University, Cambridge, Massachusetts 02138

(Received 9 February 1977)

We report measurements of semi-inclusive pion electroproduction from both hydrogen and deuterium targets carried out at the Wilson Synchrotron Laboratory at Cornell University. Measurements were made at the (W, Q^2) points (2.15 GeV, 1.2 GeV^2), (2.15, 4.0), and (3.11, 1.2) with hydrogen and deuterium, and at (2.15, 2.0), (2.67, 3.3), and (3.11, 1.7) with hydrogen only. The invariant virtual-photoproduction cross section for pions scaled by the total cross section is studied as a function of x', p_T^2, W, and Q^2. The invariant structure function shows no Q^2 dependence and a weak W dependence. The ratio of π^+ to π^- production is also presented, but a distinction between a universal ω or W dependence cannot be made.

I. INTRODUCTION

The success of the SLAC-MIT electron scattering experiments and the discovery of scaling[1] has led to a great deal of speculation about the nature of possible pointlike constituents of the proton. Over the past several years, numerous parton models[2] have been proposed to explain the data. One particular model assumes that the nucleon contains not just the usual three quarks,[3] but an infinite number of quarks distributed in momentum so that the net number of quarks is the same as in the three-quark model.[4] The electron scattering measurements carried out at the Stanford Linear Accelerator Center detect only the scattered electrons and thus measure only the total virtual-photoproduction cross section. From such experiments the momentum distribution functions of the quarks can be found.

For the semi-inclusive reactions we are concerned with here, the parton model[4] further assumes that the cross section for the production of a hadron, expressed in terms of the invariant structure function, can be written as the sum of products of parton distribution functions and parton fragmentation functions. The fragmentation function is the probability that a given type of parton will fragment into a particular hadron in the final state. The fragmentation functions are assumed to be functions only of Feynman x' while the distribution functions are assumed to be functions only of the Bjorken scaling variable $\omega = 2M\nu/Q^2$. A consequence of this model is a scaling behavior; the structure function in the forward direction depends on ω, x', and the transverse momentum p_T rather than on the center-of-mass energy W, the photon mass squared $-Q^2$, and x'.

This paper reports a study of the inclusive pion electroproduction reactions

$$e^- + p \to e^- + \pi^\pm + \text{missing mass}\ , \tag{1}$$

$$e^- + n \to e^- + \pi^\pm + \text{missing mass} \tag{2}$$

carried out at the Wilson Synchrotron Laboratory at Cornell University. The data are used to study the π^+/π^- ratio and the scaling properties of the invariant structure function. This paper represents the final report on data which have been partially described in an earlier communication.[5] A later paper will give the final report on measurements carried out at low ϵ with a different experimental set up.

II. KINEMATICS

Electroproduction can be treated as photoproduction by a virtual photon, where its mass squared $-Q^2$, energy ν, direction, and polarization parameter ϵ are tagged by the detected electron.[6] The cross sections for reactions (1) and (2) are written

$$\frac{d\sigma}{d\Omega_e dE' dp_\pi^3} = \Gamma \frac{d^3\sigma}{dp_\pi^3}\ , \tag{3}$$

where

$$\Gamma = \frac{\alpha}{4\pi^2 Q^2} \frac{E'}{E} \frac{W^2 - M^2}{M(1-\epsilon)} \tag{4}$$

and

$$\epsilon = \left[1 + 2\left(\frac{\nu^2 + Q^2}{Q^2}\right)\tan^2\left(\frac{\theta_e}{2}\right)\right]^{-1}\ . \tag{5}$$

Γ is the "flux" of virtual photons and θ_e is the electron scattering angle. $d^3\sigma/dp_\pi^3$ is the cross section for the production of a pion by a virtual photon. It is in general a function of the virtual-photon variables Q^2, ν, and ϵ, and the Feynman scaling variable x', and p_T^2. p_T is the momentum of the pion transverse to the virtual-photon direc-

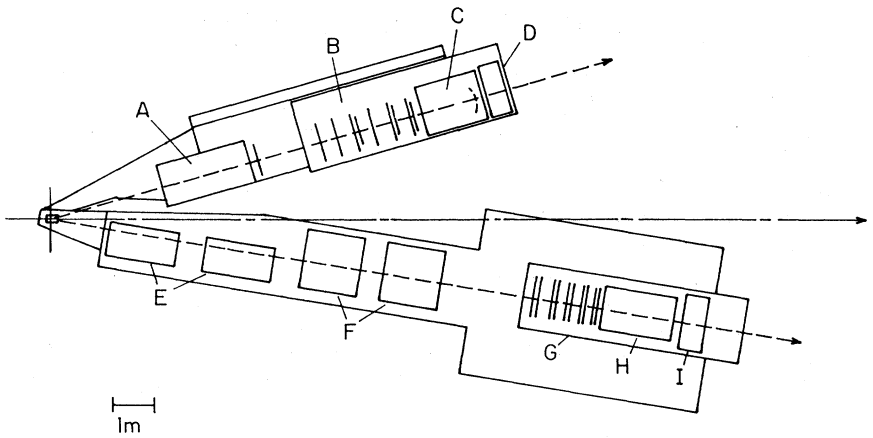

FIG. 1. A schematic diagram of the apparatus: A, 22D84 bending magnet; B, wire-spark chambers; C, Freon Čerenkov counter; D, lead-Lucite shower counter; E, 8Q48 half quadrupole magnets; F, 18D36 bending magnets; G, proportional wire chambers; H, Freon Čerenkov counter; I, lead-Lucite shower counter.

tion and x' is defined in terms of the center-of-mass momentum by

$$x' = p_L^*/[(p_{\max}^*)^2 - p_T^{\,2}]^{1/2} \ . \tag{6}$$

Here p_L^* is the component of the momentum along the virtual-photon direction and $p_{\max}^*$ is the maximum possible momentum for the pion determined by the $\pi^* n$ final state.

The data were analyzed in terms of the invariant structure function

$$F = \frac{E}{\sigma_{\rm tot}} \frac{d^3\sigma}{dp^3} = \frac{1}{\sigma_{\rm tot}} \frac{1}{\pi} \frac{E^*}{[(p_{\max}^*)^2 - p_T^{\,2}]^{1/2}} \frac{d\sigma}{dx' dp_T^{\,2}} \ , \tag{7}$$

where $\sigma_{\rm tot}$ is the total virtual-photoproduction cross section for the W and Q^2 of the reaction. $\sigma_{\rm tot}$ for the proton was taken from a fit to the SLAC-MIT measurements of νW_2 with the assumption that $\sigma_S/\sigma_T = 0.18$.[7] For the neutron, $\sigma_{\rm tot}$ was calculated from the empirical relation[8]

$$\sigma_{\rm tot}(\text{neutron}) = (1.0 - 0.75/\omega)\sigma_{\rm tot}(\text{proton}) \ . \tag{8}$$

Implicit in Eq. (7) is an average over 2π of the azimuthal angle, the angle between the electron scattering plane and the photon-hadron production plane.

III. APPARATUS

Figure 1 shows a schematic diagram of the apparatus. The apparatus was essentially the same as that used in the previously reported work carried out at the Wilson Synchrotron Laboratory.[9] The heavy-liquid shower counter used on the electron arm in the earlier experiment was replaced with a lead-lucite sandwich counter. The trigger

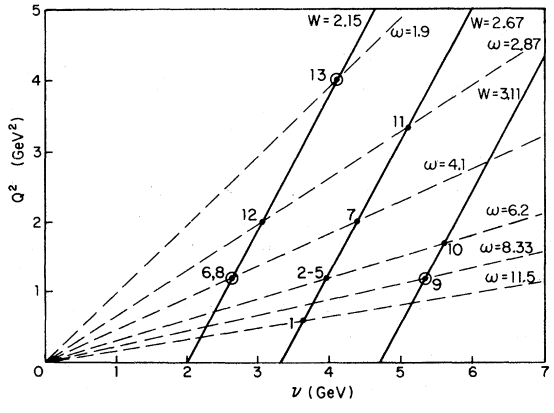

FIG. 2. The nominal (ν, Q^2) values of the points at which data were taken. The circles denote points at which deuterium data were taken.

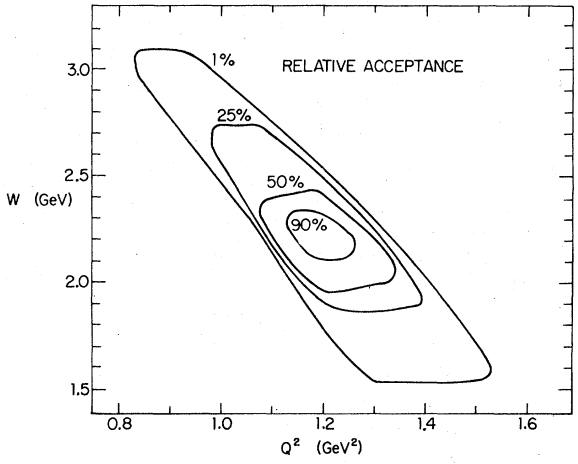

FIG. 3. The acceptance at data point 8 as a function of W and Q^2. This is typical of all the data points.

counters on the electron arm were replaced by a larger set of counters that increased the momentum acceptance from 30% to 50% [full width at half maximum (FWHM)]. The solid angle of the spectrometer was ~0.5 msr. A seventh spark chamber was placed just behind the bending magnet on the hadron arm, which increased the momentum resolution. The momentum acceptance was 60% (FWHM) and the solid angle was ~2.5 msr. The increase in the momentum acceptance of the electron arm and an increase in the available energy of the accelerator from 10 to 12 GeV enabled us to reach higher energies and momentum transfers than in the earlier experiment.

The combination of a Čerenkov counter and shower counter identified the electrons. Pions were identified by a threshold Freon-12 Čerenkov counter when their momenta were greater than 1.8 GeV and by time of flight at lower momenta. The procedure resulted in maximal separation of pions with a proton contamination of less than 1% and a loss of at most 6% of the pions due to absorption in the counters. For momenta above 5.5 GeV, both kaons and pions counted in the Čerenkov counter and could not be separated by time of flight. However, momenta above 5.5 GeV were present only in data points 9, 10, and 11 and were confined to values of x' greater than 0.85. This corresponds to the region around the $\pi^+\Delta(1236)$ final state and is not part of the inclusive region.

Figure 2 shows the virtual-photon energy, ν, and mass squared, $-Q^2$, for the points at which π^+ data were taken. Points 1–7 are from the earlier experiment[9] and points 8–13 are from this experiment. In addition to a hydrogen target, a deuterium target was used at points 8, 9, and 13, which are circled in Fig. 2. π^- data were taken at points 8, 9, and 13 from both targets and also at points 10 and 12 from hydrogen.

The acceptance of the apparatus was such that W and Q^2 were correlated. Figure 3 shows the acceptance at data point 8 which is typical of all the data points. The W distribution was about 0.5 GeV wide (FWHM) and the Q^2 distribution was about 0.25 GeV^2 wide for p_T^2 restricted to less than 0.02 GeV^2.

A Monte Carlo calculation assuming unit center-of-mass cross section and incorporating multiple-scattering, detector-resolution, and geometrical effects was used to determine the acceptance. The program randomly generated events to uniformly fill the acceptance of the two spectrometers. The Monte Carlo events were then analyzed with exactly the same procedures used for the data. The statistical error for each bin includes the uncertainty due to the number of Monte Carlo events in that bin. There were always at least four times as many Monte Carlo events as data events to keep the contribution to the statistical error due to the Monte Carlo events below 10%.

IV. CALIBRATION

The normalization of the experiment was checked by independently observing elastically scattered electrons in both spectrometers and comparing the observed cross sections with the measured elastic scattering cross section. The Monte Carlo determination of the acceptance indicated that the resolution in angle and momentum was multiple-scattering dominated. The ratio of the measured elastic scattering cross section to the average world data was 0.994 ± 0.007 and 0.998 ± 0.009 for the electron and hadron spectrometers, respectively.

V. CORRECTIONS

The data have been corrected for random coincidences [~(5 ± 1)%], counter and spark-chamber dead time [~(5 ± 2)%], spark-chamber inefficiency [(1 ± 0.5)%], target-wall background [~(5 ± 2)%], absorption in the counters [(2 ± 1)% to (6 ± 3 %], decay losses [about (30 ± 3)% at the lowest momenta and (2 ± 0.2)% at the highest], and electron misidentification [0% to (3 ± 1)%]. The errors quoted are statistical only. We estimate the overall systematic error to be less than 10%. This systematic uncertainty reflects the uncertainty in the corrections applied to the data.

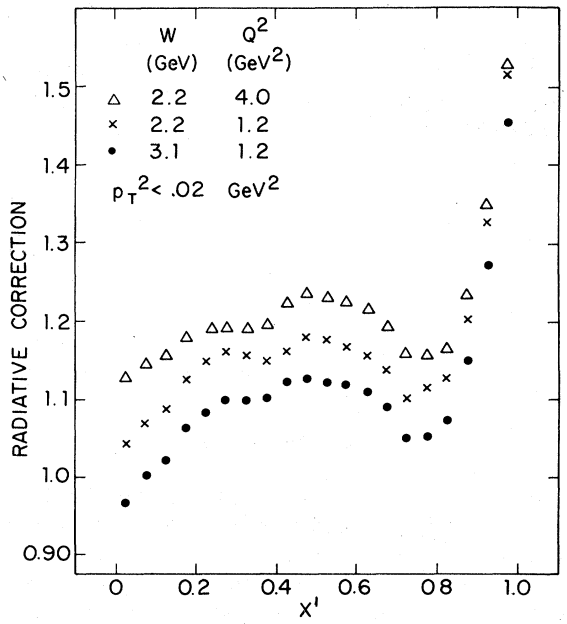

FIG. 4. The radiative correction as a function of W, Q^2, and x' for $p_T^2 < 0.02$ GeV^2.

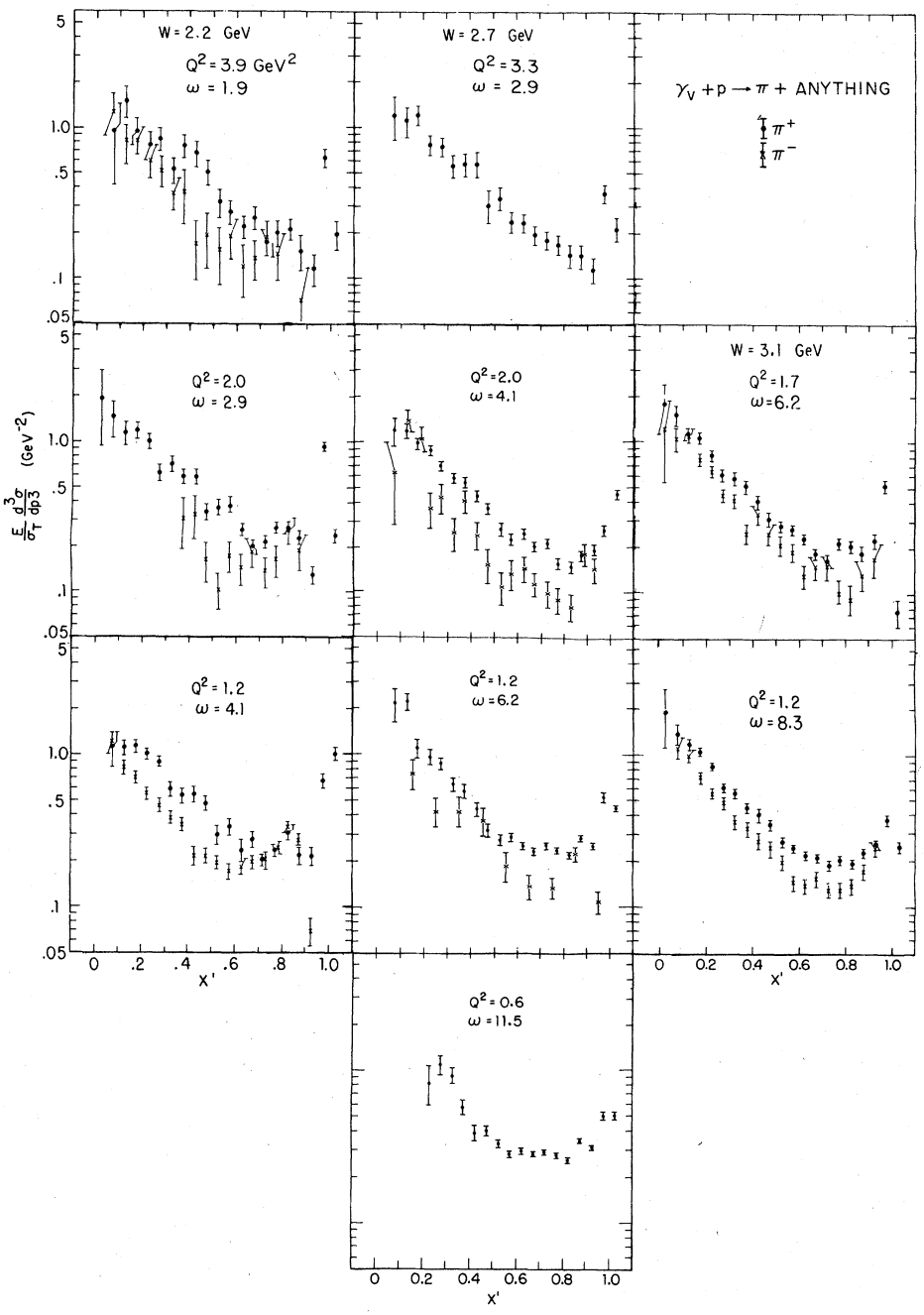

FIG. 5. The structure functions from the hydrogen target for $p_T^2 < 0.02$ GeV^2.

A. Deuteron corrections

The deuterium data were analyzed with the assumption that the cross section for the deuteron is the simple sum of the cross sections for the proton and neutron; the proton and neutron in the deuteron are treated as free particles. A correction was then made for the Fermi motion of the nucleons in the deuteron. The correction factor was determined by a Monte Carlo calculation assuming that the nucleons were on the mass shell and had a momentum distribution given by the Hulthén momentum wave function.[10] Using the measured structure function, F, for the production of pions in the forward direction from a proton target and data from other experiments[11] in the backward direction, a smeared pion structure function, F_s, was calculated. The smearing correction was

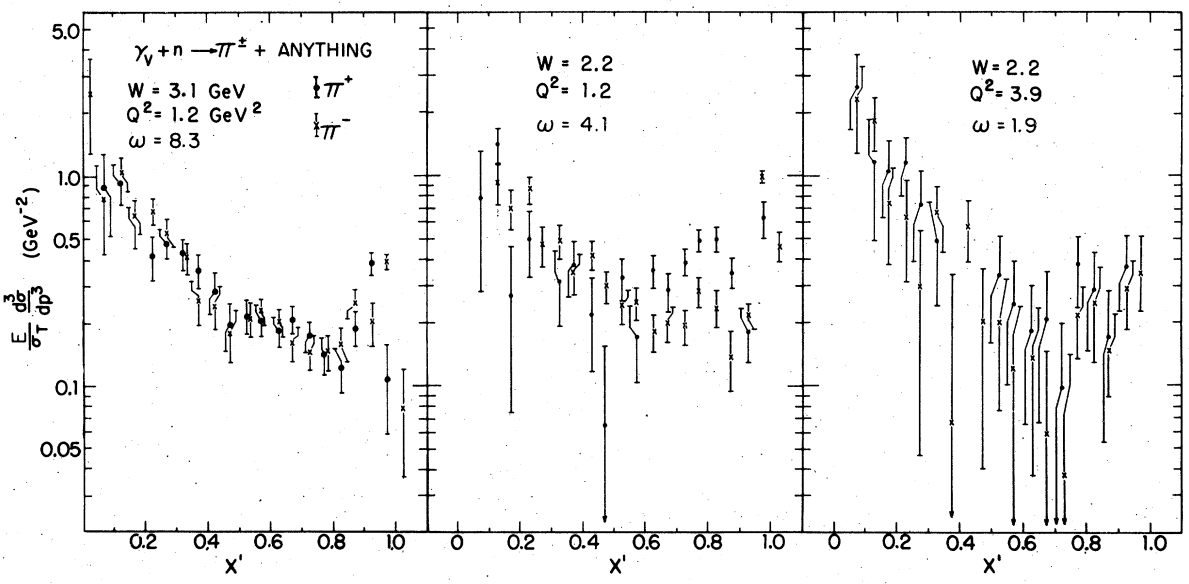

FIG. 6. The structure functions from neutrons for $p_T^2 < 0.02$ GeV^2.

the ratio of the unsmeared to smeared structure functions. It differed from unity by less than 3% at all the data points. Assuming that the smearing affects the neutron and proton in the same way, the unsmeared neutron cross section was extracted from the deuterium data according to

$$F_n = \frac{1}{\sigma_{\text{tot}}^n}\left[\left(\frac{F}{F_s}\right)\frac{d^3\sigma}{dp^3}\bigg|_D - \frac{d^3\sigma}{dp^3}\bigg|_H\right]. \quad (9)$$

An estimate was made for the geometrical

TABLE I. The π^+ proton structure function for $p_T^2 < 0.02$ GeV^2 as a function of x' for various W and Q^2. Rad corr is the radiative correction used to convert the measured structure functions to the F values shown in the table. N is the number of events that contributed to the bin. The x' bin size is 0.05.

x'	F (GeV^{-2})	W (GeV)	Q^2 (GeV^2)	ϵ	p_T^2 (GeV^2)	ω	σ_{tot} (μb)	Rad corr	N
			(a) Data point 8: $W = 2.2$ GeV, $Q^2 = 1.2$ GeV^2						
0.080	1.184 ± 0.307	2.76	0.99	0.86	0.0063	7.99	44.62	1.065	92
0.125	1.211 ± 0.139	2.60	1.06	0.89	0.0074	6.77	44.46	1.096	254
0.174	1.241 ± 0.113	2.44	1.11	0.91	0.0074	5.78	44.87	1.098	374
0.225	1.154 ± 0.101	2.28	1.16	0.93	0.0068	4.92	44.59	1.147	356
0.273	1.072 ± 0.092	2.20	1.19	0.94	0.0056	4.45	46.15	1.200	322
0.325	0.658 ± 0.074	2.08	1.23	0.95	0.0077	3.94	46.82	1.118	249
0.374	0.619 ± 0.070	2.09	1.24	0.95	0.0072	3.91	46.37	1.160	193
0.425	0.632 ± 0.071	2.10	1.23	0.95	0.0089	3.94	46.64	1.159	174
0.476	0.569 ± 0.067	2.12	1.22	0.95	0.0103	4.04	46.17	1.189	141
0.523	0.345 ± 0.048	2.20	1.20	0.94	0.0097	4.33	45.34	1.166	101
0.576	0.389 ± 0.048	2.15	1.20	0.95	0.0089	4.17	46.11	1.162	105
0.625	0.271 ± 0.040	2.18	1.20	0.94	0.0098	4.28	45.80	1.165	90
0.676	0.312 ± 0.038	2.18	1.20	0.94	0.0088	4.26	45.83	1.129	94
0.722	0.227 ± 0.030	2.14	1.21	0.95	0.0083	4.10	45.88	1.120	80
0.775	0.260 ± 0.030	2.14	1.22	0.95	0.0102	4.08	45.88	1.091	99
0.824	0.351 ± 0.040	2.14	1.22	0.95	0.0089	4.05	45.70	1.144	113
0.875	0.261 ± 0.033	2.14	1.21	0.95	0.0097	4.09	46.09	1.204	84
0.921	0.269 ± 0.036	2.16	1.21	0.94	0.0088	4.16	45.71	1.262	75
0.985	1.014 ± 0.108	2.12	1.22	0.95	0.0091	3.98	45.85	1.515	190
1.012	1.526 ± 0.150	2.12	1.21	0.95	0.0096	4.00	46.19	1.515	296

TABLE I. (*Continued*)

x'	F (GeV^{-2})	W (GeV)	Q^2 (GeV^2)	ϵ	p_T^2 (GeV^2)	ω	σ_{tot} (μb)	Rad corr	N
			(b) Data point 9: $W=3.1$ GeV, $Q^2=1.2$ GeV^2						
0.045	1.915 ± 0.795	3.30	1.09	0.76	0.0004	10.40	37.53	0.965	7
0.081	1.419 ± 0.211	3.08	1.20	0.81	0.0013	8.67	36.71	1.007	91
0.127	1.232 ± 0.102	3.09	1.20	0.81	0.0025	8.68	36.60	1.033	282
0.177	1.103 ± 0.068	3.03	1.23	0.82	0.0047	8.34	36.56	1.027	484
0.223	0.948 ± 0.056	3.02	1.24	0.83	0.0064	8.07	36.36	1.092	490
0.274	0.706 ± 0.047	3.02	1.24	0.83	0.0079	7.99	36.33	1.128	393
0.324	0.608 ± 0.042	3.02	1.24	0.83	0.0092	7.95	36.24	1.057	320
0.374	0.517 ± 0.041	3.06	1.22	0.82	0.0096	8.19	36.32	1.119	237
0.426	0.452 ± 0.041	3.09	1.20	0.82	0.0105	8.47	36.58	1.104	187
0.475	0.408 ± 0.032	3.15	1.17	0.80	0.0110	8.95	36.72	1.148	228
0.526	0.304 ± 0.021	3.18	1.15	0.80	0.0105	9.14	36.81	1.107	272
0.575	0.273 ± 0.018	3.17	1.16	0.80	0.0095	9.03	36.69	1.102	333
0.626	0.253 ± 0.016	3.14	1.17	0.81	0.0085	8.76	36.62	1.134	363
0.676	0.230 ± 0.014	3.11	1.19	0.81	0.0095	8.50	36.41	1.076	349
0.724	0.204 ± 0.013	3.10	1.20	0.82	0.0100	8.40	36.41	1.067	318
0.774	0.214 ± 0.013	3.10	1.20	0.82	0.0096	8.39	36.37	1.026	347
0.824	0.214 ± 0.014	3.10	1.20	0.82	0.0093	8.40	36.40	1.087	313
0.875	0.272 ± 0.019	3.10	1.20	0.82	0.0095	8.33	36.29	1.169	299
0.924	0.314 ± 0.023	3.09	1.21	0.82	0.0091	8.19	36.11	1.198	288
0.986	0.552 ± 0.037	3.05	1.22	0.83	0.0096	7.96	36.23	1.454	376
1.005	0.371 ± 0.034	3.07	1.21	0.83	0.0090	8.09	36.31	1.454	177
			(c) Data point 10: $W=3.1$ GeV, $Q^2=1.7$ GeV^2						
0.039	1.772 ± 0.635	3.13	1.65	0.77	0.0007	6.90	28.59	0.977	16
0.080	1.551 ± 0.238	3.09	1.71	0.78	0.0015	6.44	27.94	1.016	115
0.128	1.188 ± 0.121	3.07	1.73	0.79	0.0029	6.29	27.91	1.044	202
0.174	1.121 ± 0.088	3.02	1.77	0.80	0.0054	6.04	27.63	1.038	289
0.226	0.912 ± 0.075	3.05	1.74	0.79	0.0075	6.17	27.82	1.099	283
0.275	0.696 ± 0.062	3.08	1.73	0.79	0.0083	6.20	27.83	1.135	249
0.323	0.620 ± 0.056	3.07	1.73	0.79	0.0084	6.10	27.88	1.060	219
0.374	0.574 ± 0.058	3.08	1.73	0.79	0.0089	6.12	27.78	1.124	161
0.425	0.452 ± 0.047	3.10	1.71	0.78	0.0116	6.28	27.89	1.110	134
0.476	0.362 ± 0.038	3.19	1.65	0.77	0.0133	6.74	28.31	1.156	184
0.526	0.314 ± 0.027	3.16	1.66	0.77	0.0099	6.59	28.22	1.114	221
0.575	0.293 ± 0.022	3.15	1.68	0.78	0.0091	6.45	28.02	1.110	261
0.622	0.265 ± 0.020	3.13	1.70	0.78	0.0086	6.30	27.95	1.142	266
0.676	0.200 ± 0.018	3.11	1.71	0.79	0.0091	6.20	27.90	1.082	221
0.726	0.179 ± 0.017	3.11	1.70	0.79	0.0095	6.21	27.96	1.073	206
0.774	0.222 ± 0.018	3.11	1.70	0.79	0.0096	6.23	27.99	1.031	223
0.824	0.226 ± 0.020	3.11	1.70	0.79	0.0097	6.21	27.96	1.089	183
0.875	0.217 ± 0.022	3.10	1.72	0.79	0.0088	6.13	27.80	1.167	145
0.924	0.270 ± 0.029	3.09	1.72	0.79	0.0082	6.06	27.83	1.196	143
0.986	0.758 ± 0.066	3.07	1.73	0.80	0.0088	5.96	27.72	1.458	261
1.002	0.110 ± 0.023	3.08	1.72	0.80	0.0081	6.02	27.86	1.458	27

TABLE I. (*Continued*)

x'	F (GeV^{-2})	W (GeV)	Q^2 (GeV^2)	ϵ	p_T^2 (GeV^2)	ω	σ_{tot} (μb)	Rad corr	N
			(d) Data point 11: $W=2.7$ GeV, $Q^2=3.3$ GeV^2						
0.082	1.293 ± 0.416	2.76	3.18	0.80	0.0018	3.23	16.04	1.074	21
0.127	1.217 ± 0.280	2.76	3.19	0.80	0.0035	3.21	15.95	1.099	51
0.173	1.309 ± 0.197	2.74	3.21	0.80	0.0054	3.16	15.83	1.087	78
0.222	0.882 ± 0.137	2.73	3.22	0.80	0.0080	3.16	15.80	1.151	65
0.273	0.883 ± 0.128	2.68	3.26	0.81	0.0093	3.02	15.57	1.180	64
0.322	0.617 ± 0.105	2.62	3.35	0.83	0.0090	2.84	15.10	1.105	44
0.369	0.658 ± 0.115	2.69	3.26	0.82	0.0095	2.99	15.67	1.162	45
0.426	0.664 ± 0.130	2.66	3.34	0.82	0.0097	2.90	15.25	1.154	36
0.476	0.366 ± 0.091	2.69	3.28	0.82	0.0106	2.97	15.60	1.197	21
0.531	0.393 ± 0.068	2.74	3.22	0.81	0.0108	3.08	15.98	1.163	46
0.573	0.276 ± 0.044	2.75	3.20	0.81	0.0097	3.10	16.08	1.160	57
0.626	0.274 ± 0.038	2.68	3.31	0.82	0.0098	2.92	15.45	1.178	63
0.676	0.220 ± 0.030	2.68	3.28	0.82	0.0089	2.95	15.64	1.129	75
0.723	0.200 ± 0.028	2.67	3.31	0.82	0.0093	2.91	15.48	1.117	62
0.775	0.181 ± 0.026	2.67	3.30	0.82	0.0105	2.91	15.56	1.075	61
0.820	0.161 ± 0.029	2.67	3.30	0.82	0.0094	2.91	15.52	1.128	43
0.876	0.169 ± 0.029	2.70	3.29	0.81	0.0095	2.97	15.62	1.198	44
0.922	0.142 ± 0.027	2.67	3.29	0.82	0.0099	2.91	15.58	1.237	33
0.991	0.541 ± 0.074	2.66	3.33	0.82	0.0101	2.87	15.37	1.480	83
1.003	0.313 ± 0.057	2.66	3.30	0.82	0.0089	2.89	15.52	1.480	41
			(e) Data point 12: $W=2.2$ GeV, $Q^2=2.0$ GeV^2						
0.081	1.643 ± 0.381	2.65	1.73	0.89	0.0054	4.64	29.99	1.107	48
0.124	1.297 ± 0.227	2.48	1.80	0.91	0.0056	4.04	29.98	1.135	101
0.177	1.347 ± 0.156	2.38	1.87	0.92	0.0060	3.64	29.27	1.134	146
0.224	1.187 ± 0.134	2.31	1.90	0.92	0.0067	3.43	29.17	1.188	162
0.275	0.724 ± 0.093	2.25	1.93	0.93	0.0075	3.26	29.05	1.145	132
0.324	0.819 ± 0.091	2.20	1.97	0.94	0.0075	3.07	28.76	1.149	142
0.375	0.699 ± 0.078	2.16	1.96	0.94	0.0077	2.97	28.99	1.193	114
0.425	0.703 ± 0.082	2.14	1.98	0.94	0.0087	2.92	28.69	1.191	109
0.475	0.419 ± 0.056	2.19	1.97	0.94	0.0101	3.03	28.79	1.224	99
0.527	0.439 ± 0.048	2.22	1.94	0.94	0.0105	3.10	29.05	1.200	116
0.573	0.453 ± 0.046	2.23	1.94	0.93	0.0102	3.13	29.08	1.198	153
0.625	0.312 ± 0.031	2.19	1.97	0.94	0.0082	3.00	28.84	1.201	146
0.676	0.232 ± 0.025	2.18	1.97	0.94	0.0089	3.00	28.90	1.164	126
0.724	0.249 ± 0.025	2.18	1.98	0.94	0.0085	2.97	28.73	1.151	141
0.775	0.298 ± 0.027	2.14	1.99	0.94	0.0092	2.86	28.71	1.118	173
0.824	0.316 ± 0.028	2.15	1.99	0.94	0.0084	2.88	28.64	1.167	177
0.873	0.283 ± 0.027	2.16	1.98	0.94	0.0088	2.93	28.85	1.228	152
0.925	0.168 ± 0.022	2.14	2.00	0.94	0.0089	2.87	28.53	1.288	78
0.988	1.427 ± 0.098	2.12	2.00	0.94	0.0096	2.83	28.58	1.527	503
1.005	0.363 ± 0.040	2.14	1.98	0.94	0.0087	2.86	28.78	1.527	118

TABLE I. (*Continued*)

x'	F (GeV^{-2})	W (GeV)	Q^2 (GeV^2)	ϵ	p_T^2 (GeV^2)	ω	σ_{tot} (μb)	Rad corr	N
			(f) Data point 13: $W=2.2$ GeV, $Q^2=4.0$ GeV^2						
0.077	1.057 ± 0.583	2.63	3.47	0.82	0.0047	2.78	14.44	1.139	16
0.129	1.767 ± 0.401	2.48	3.64	0.84	0.0052	2.51	13.39	1.167	54
0.173	1.086 ± 0.222	2.44	3.68	0.85	0.0067	2.41	13.04	1.159	59
0.224	0.925 ± 0.196	2.31	3.79	0.86	0.0065	2.22	12.19	1.212	56
0.275	0.993 ± 0.176	2.28	3.83	0.87	0.0065	2.16	11.86	1.195	53
0.325	0.601 ± 0.118	2.20	3.90	0.87	0.0083	2.06	11.26	1.165	39
0.375	0.912 ± 0.158	2.16	3.94	0.88	0.0084	1.99	10.99	1.214	49
0.421	0.809 ± 0.158	2.14	3.99	0.88	0.0098	1.96	10.64	1.212	39
0.478	0.623 ± 0.119	2.19	3.93	0.88	0.0100	2.02	11.09	1.247	36
0.526	0.389 ± 0.084	2.20	3.96	0.88	0.0110	2.01	11.01	1.223	30
0.578	0.333 ± 0.062	2.23	3.92	0.87	0.0080	2.05	11.33	1.221	37
0.622	0.267 ± 0.046	2.20	3.95	0.88	0.0083	2.02	11.11	1.223	40
0.674	0.295 ± 0.052	2.20	3.92	0.88	0.0097	2.02	11.22	1.186	54
0.729	0.202 ± 0.038	2.10	4.03	0.89	0.0111	1.89	10.28	1.173	32
0.776	0.224 ± 0.044	2.15	3.96	0.88	0.0090	1.96	10.86	1.135	46
0.825	0.245 ± 0.040	2.12	4.00	0.88	0.0091	1.91	10.54	1.180	46
0.871	0.186 ± 0.050	2.16	3.96	0.88	0.0097	1.96	10.85	1.238	29
0.922	0.147 ± 0.035	2.15	3.95	0.88	0.0119	1.96	10.88	1.283	20
0.987	0.947 ± 0.125	2.13	4.01	0.88	0.0094	1.92	10.54	1.526	102
1.006	0.295 ± 0.064	2.15	3.94	0.88	0.0116	1.95	10.93	1.526	29

TABLE II. The π^- proton structure function for $p_T^2 < 0.02$ GeV^2 as a function of x' for various W and Q^2.

x'	F (GeV^{-2})	W (GeV)	Q^2 (GeV^2)	ϵ	p_T^2 (GeV^2)	ω	σ_{tot} (μb)	Rad corr	N
			(a) Data point 8: $W=2.2$ GeV, $Q^2=1.2$ GeV^2						
0.081	1.306 ± 0.218	2.78	0.98	0.86	0.0073	8.11	44.39	1.094	101
0.128	0.910 ± 0.100	2.59	1.06	0.89	0.0072	6.71	44.37	1.114	255
0.176	0.781 ± 0.071	2.45	1.11	0.91	0.0072	5.82	44.82	1.107	317
0.224	0.636 ± 0.062	2.29	1.17	0.93	0.0064	4.92	45.16	1.155	314
0.275	0.548 ± 0.056	2.24	1.18	0.93	0.0066	4.64	45.70	1.179	312
0.324	0.435 ± 0.040	2.17	1.21	0.94	0.0079	4.30	45.92	1.134	267
0.376	0.407 ± 0.038	2.15	1.20	0.94	0.0081	4.23	46.26	1.179	254
0.425	0.253 ± 0.035	2.18	1.20	0.94	0.0087	4.30	46.01	1.174	200
0.476	0.258 ± 0.029	2.16	1.21	0.94	0.0097	4.22	45.94	1.198	182
0.526	0.228 ± 0.024	2.16	1.21	0.94	0.0090	4.22	45.81	1.172	180
0.574	0.200 ± 0.024	2.15	1.22	0.95	0.0085	4.12	45.64	1.175	161
0.623	0.216 ± 0.023	2.16	1.20	0.94	0.0086	4.18	45.93	1.184	170
0.674	0.223 ± 0.022	2.13	1.22	0.95	0.0086	4.04	46.04	1.151	167
0.727	0.228 ± 0.022	2.13	1.22	0.95	0.0094	4.05	46.01	1.137	180
0.778	0.268 ± 0.025	2.12	1.21	0.95	0.0089	4.01	46.32	1.100	215
0.825	0.391 ± 0.032	2.12	1.21	0.95	0.0098	4.00	46.27	1.182	274
0.871	0.354 ± 0.032	2.15	1.21	0.95	0.0094	4.11	45.97	1.300	199
0.915	0.098 ± 0.020	2.16	1.20	0.95	0.0093	4.19	46.07	1.410	48
0.971	0.034 ± 0.013	2.12	1.21	0.95	0.0090	4.03	46.25	1.636	12

TABLE II. (*Continued*)

x'	F (GeV^{-2})	W (GeV)	Q^2 (GeV^2)	ϵ	p_T^2 (GeV^2)	ω	σ_{tot} (μb)	Rad corr	N
			(b) Data point 9: $W=3.1$ GeV, $Q^2=1.2$ GeV^2						
0.082	1.189 ± 0.190	3.06	1.21	0.81	0.0016	8.62	36.73	1.025	67
0.127	1.047 ± 0.103	3.06	1.21	0.81	0.0026	8.56	36.73	1.040	194
0.177	0.747 ± 0.064	2.99	1.25	0.83	0.0050	7.97	36.36	1.025	236
0.223	0.625 ± 0.052	2.98	1.25	0.83	0.0066	7.81	36.38	1.089	228
0.272	0.561 ± 0.051	3.05	1.22	0.82	0.0076	8.30	36.50	1.130	202
0.324	0.396 ± 0.041	3.01	1.26	0.83	0.0090	7.81	35.97	1.063	145
0.374	0.379 ± 0.040	3.05	1.23	0.83	0.0092	8.07	36.29	1.128	138
0.424	0.311 ± 0.038	3.07	1.21	0.82	0.0103	8.30	36.47	1.108	102
0.474	0.283 ± 0.034	3.17	1.17	0.80	0.0103	9.04	36.63	1.148	99
0.524	0.222 ± 0.025	3.16	1.17	0.80	0.0098	8.96	36.62	1.104	117
0.577	0.162 ± 0.019	3.16	1.17	0.80	0.0092	8.89	36.57	1.104	100
0.624	0.160 ± 0.019	3.12	1.19	0.81	0.0092	8.57	36.50	1.144	112
0.673	0.170 ± 0.019	3.12	1.19	0.81	0.0100	8.52	36.34	1.089	125
0.722	0.143 ± 0.016	3.13	1.18	0.81	0.0078	8.66	36.61	1.076	108
0.775	0.136 ± 0.016	3.10	1.20	0.82	0.0092	8.35	36.41	1.027	111
0.825	0.155 ± 0.019	3.11	1.20	0.82	0.0085	8.35	36.16	1.118	97
0.876	0.219 ± 0.025	3.09	1.19	0.82	0.0089	9.34	36.47	1.251	113
0.923	0.328 ± 0.036	3.10	1.20	0.82	0.0097	8.35	36.43	1.327	150
0.956	0.037 ± 0.015	3.13	1.15	0.82	0.0080	8.74	37.09	1.553	11
			(c) Data point 10: $W=3.1$ GeV, $Q^2=1.7$ GeV^2						
0.043	1.222 ± 0.660	3.01	1.77	0.80	0.0005	5.95	27.69	0.996	10
0.079	1.104 ± 0.191	3.11	1.71	0.78	0.0009	6.36	27.88	1.032	70
0.126	1.169 ± 0.116	3.03	1.77	0.80	0.0030	6.02	27.57	1.048	175
0.174	0.803 ± 0.076	3.04	1.74	0.79	0.0047	6.13	27.83	1.035	205
0.225	0.714 ± 0.061	3.06	1.73	0.79	0.0078	6.21	27.89	1.095	218
0.275	0.509 ± 0.051	3.07	1.73	0.79	0.0079	6.18	27.86	1.136	176
0.321	0.442 ± 0.047	3.07	1.74	0.79	0.0086	6.07	27.71	1.066	144
0.374	0.286 ± 0.043	3.07	1.73	0.80	0.0098	6.06	27.84	1.132	90
0.426	0.376 ± 0.052	3.10	1.73	0.79	0.0103	6.17	27.71	1.114	81
0.475	0.289 ± 0.045	3.13	1.68	0.78	0.0105	6.41	28.11	1.155	71
0.526	0.234 ± 0.034	3.17	1.66	0.77	0.0108	6.61	28.21	1.111	71
0.575	0.211 ± 0.030	3.11	1.72	0.79	0.0094	6.19	27.79	1.111	76
0.627	0.152 ± 0.026	3.12	1.69	0.79	0.0086	6.28	27.99	1.150	53
0.673	0.167 ± 0.028	3.10	1.70	0.79	0.0090	6.18	28.08	1.095	53
0.724	0.166 ± 0.028	3.10	1.72	0.79	0.0102	6.11	27.72	1.081	53
0.777	0.104 ± 0.024	3.08	1.72	0.80	0.0096	6.03	27.82	1.031	32
0.825	0.105 ± 0.023	3.10	1.69	0.79	0.0099	6.25	28.15	1.118	30
0.877	0.170 ± 0.037	3.10	1.70	0.79	0.0091	6.15	28.01	1.251	32
0.925	0.229 ± 0.058	3.11	1.68	0.79	0.0097	6.26	28.22	1.327	30
			(d) Data point 12: $W=2.2$ GeV, $Q^2=4.0$ GeV^2						
0.367	0.371 ± 0.138	2.43	1.86	0.92	0.0138	3.70	29.53	1.208	10
0.425	0.397 ± 0.129	2.34	1.93	0.92	0.0101	3.40	28.82	1.203	16
0.474	0.201 ± 0.059	2.21	1.97	0.94	0.0082	3.06	28.74	1.230	17
0.521	0.124 ± 0.034	2.23	1.91	0.94	0.0080	3.17	29.63	1.203	16
0.575	0.209 ± 0.048	2.19	1.97	0.94	0.0084	3.01	28.80	1.204	24
0.622	0.175 ± 0.042	2.18	1.96	0.94	0.0094	3.00	29.11	1.214	22
0.675	0.219 ± 0.048	2.13	1.98	0.94	0.0081	2.88	28.93	1.178	28
0.721	0.159 ± 0.037	2.13	1.98	0.94	0.0107	2.87	28.84	1.161	24
0.774	0.183 ± 0.043	2.08	2.02	0.95	0.0096	2.73	28.49	1.122	24
0.821	0.310 ± 0.068	2.10	2.01	0.94	0.0095	2.78	28.53	1.199	33
0.872	0.250 ± 0.067	2.14	1.98	0.94	0.0083	2.87	28.83	1.317	20

TABLE II. (*Continued*)

x'	F (GeV^{-2})	W (GeV)	Q^2 (GeV^2)	ϵ	p_T^2 (GeV^2)	ω	σ_{tot} (μb)	Rad corr	N
			(e) Data point 13: $W=2.2$ GeV, $Q^2=4.0$ GeV^2						
0.079	1.478 ± 0.467	2.67	3.44	0.81	0.0054	2.85	14.63	1.155	13
0.126	0.943 ± 0.277	2.51	3.62	0.84	0.0050	2.52	13.48	1.181	27
0.175	0.960 ± 0.198	2.35	3.74	0.86	0.0067	2.31	12.46	1.166	36
0.223	0.732 ± 0.177	2.35	3.79	0.86	0.0086	2.28	12.26	1.218	30
0.274	0.642 ± 0.151	2.18	3.90	0.88	0.0091	2.05	11.04	1.240	23
0.324	0.436 ± 0.105	2.27	3.83	0.87	0.0097	2.14	11.84	1.175	22
0.376	0.456 ± 0.179	2.17	3.99	0.88	0.0110	1.99	10.70	1.228	15
0.419	0.206 ± 0.088	2.24	3.95	0.87	0.0079	2.05	11.21	1.223	7
0.474	0.240 ± 0.097	2.18	3.94	0.88	0.0109	2.01	10.97	1.253	10
0.523	0.187 ± 0.077	2.21	3.86	0.88	0.0070	2.06	11.51	1.226	7
0.577	0.230 ± 0.067	2.22	3.90	0.87	0.0085	2.06	11.39	1.226	14
0.620	0.146 ± 0.055	2.20	3.96	0.88	0.0089	2.01	11.03	1.233	11
0.675	0.161 ± 0.046	2.13	3.97	0.88	0.0091	1.93	10.68	1.197	14
0.717	0.219 ± 0.059	2.10	4.03	0.89	0.0080	1.88	10.24	1.178	17
0.768	0.166 ± 0.057	2.13	4.04	0.88	0.0087	1.91	10.37	1.136	10

shadowing of one nucleon by the other.[12] This was found to be a less than 0.1% correction to F_n.

B. Radiative corrections

Corrections for the radiation of soft photons were calculated using the equivalent-radiator method of Mo and Tsai.[13] It was assumed that only the electrons radiated. Radiation by hadrons and the interference between hadron and electron radiation was ignored. The correction was calculated by first assuming that the measured cross section contained no radiative effects and calculating from it a radiated cross section. The measured cross

TABLE III. The π^+ neutron structure function for $p_T^2 < 0.02$ GeV^2 as a function of x' for various W and Q^2. σ_{tot} is the proton virtual-photoproduction total cross section.

x'	F (GeV^{-2})	W (GeV)	Q^2 (GeV^2)	ϵ	p_T^2 (GeV^2)	ω	σ_{tot} (μb)	Rad corr	N
			(a) Data point 8: $W=2.2$ GeV, $Q^2=1.2$ GeV^2						
0.084	0.841 ± 0.539	2.73	0.98	0.87	0.0064	7.87	45.09	1.065	103
0.125	1.543 ± 0.310	2.57	1.04	0.89	0.0069	6.76	45.28	1.096	304
0.176	0.296 ± 0.213	2.45	1.08	0.91	0.0074	5.94	45.71	1.098	314
0.224	0.574 ± 0.197	2.30	1.13	0.93	0.0063	5.08	46.34	1.147	365
0.275	0.016 ± 0.171	2.22	1.16	0.94	0.0067	4.65	46.70	1.200	311
0.325	0.351 ± 0.136	2.19	1.17	0.94	0.0070	4.47	46.71	1.118	313
0.373	0.436 ± 0.128	2.17	1.18	0.94	0.0075	4.37	46.79	1.160	310
0.425	0.256 ± 0.120	2.20	1.18	0.94	0.0086	4.42	46.26	1.159	308
0.476	0.078 ± 0.107	2.18	1.18	0.94	0.0087	4.35	46.66	1.189	275
0.525	0.381 ± 0.087	2.17	1.19	0.94	0.0091	4.29	46.15	1.166	309
0.577	0.199 ± 0.080	2.17	1.19	0.94	0.0090	4.28	46.23	1.162	274
0.624	0.411 ± 0.074	2.16	1.20	0.94	0.0083	4.20	46.28	1.165	312
0.675	0.319 ± 0.067	2.15	1.20	0.95	0.0086	4.14	46.13	1.129	319
0.726	0.434 ± 0.061	2.12	1.20	0.95	0.0089	4.06	46.58	1.120	343
0.775	0.538 ± 0.065	2.13	1.21	0.95	0.0089	4.06	46.36	1.091	386
0.825	0.574 ± 0.078	2.14	1.20	0.95	0.0089	4.11	46.16	1.144	428
0.873	0.418 ± 0.067	2.15	1.20	0.95	0.0084	4.13	46.12	1.204	278
0.925	0.228 ± 0.065	2.12	1.20	0.95	0.0097	4.01	46.55	1.262	192
0.981	0.950 ± 0.188	2.12	1.21	0.95	0.0089	4.01	46.38	1.515	533

TABLE III. (*Continued*)

x'	F (GeV^{-2})	W (GeV)	Q^2 (GeV^2)	ϵ	p_T^2 (GeV^2)	ω	σ_{tot} (μb)	Rad corr	N
			(b) Data point 9: $W=3.1$ GeV, $Q^2=1.2$ GeV^2						
0.082	0.884 ± 0.368	3.01	1.23	0.82	0.0015	8.23	36.67	1.007	158
0.128	0.939 ± 0.203	3.02	1.23	0.82	0.0027	8.21	36.59	1.033	384
0.176	0.588 ± 0.131	3.01	1.23	0.82	0.0048	8.20	36.65	1.027	562
0.266	0.488 ± 0.105	3.04	1.21	0.82	0.0062	8.37	36.78	1.092	601
0.275	0.535 ± 0.087	3.06	1.20	0.82	0.0073	8.43	36.86	1.128	604
0.324	0.446 ± 0.076	3.05	1.20	0.82	0.0081	8.29	36.71	1.057	558
0.373	0.396 ± 0.075	3.04	1.21	0.83	0.0082	8.14	36.62	1.119	444
0.424	0.309 ± 0.069	3.06	1.20	0.82	0.0094	8.29	36.63	1.104	341
0.475	0.225 ± 0.058	3.10	1.18	0.81	0.0108	8.59	36.77	1.148	295
0.526	0.237 ± 0.044	3.14	1.16	0.81	0.0107	8.90	36.97	1.107	321
0.575	0.226 ± 0.039	3.14	1.16	0.81	0.0096	8.86	36.97	1.102	340
0.626	0.206 ± 0.034	3.11	1.18	0.81	0.0091	8.58	36.69	1.134	349
0.675	0.222 ± 0.033	3.10	1.18	0.82	0.0090	8.49	36.69	1.076	359
0.725	0.185 ± 0.030	3.09	1.19	0.82	0.0093	8.35	36.64	1.067	317
0.774	0.144 ± 0.029	3.10	1.18	0.82	0.0093	8.49	36.84	1.026	303
0.826	0.133 ± 0.031	3.09	1.18	0.82	0.0097	8.46	36.83	1.087	242
0.876	0.220 ± 0.043	3.08	1.18	0.82	0.0096	8.36	36.80	1.169	267
0.924	0.456 ± 0.057	3.08	1.19	0.82	0.0094	8.26	36.56	1.198	384
0.982	0.158 ± 0.073	3.06	1.20	0.83	0.0092	8.09	36.52	1.454	236
			(c) Data point 13: $W=2.2$ GeV, $Q^2=4.0$ GeV^2						
0.081	3.067 ± 1.202	2.58	3.49	0.83	0.0042	2.70	14.26	1.139	60
0.127	1.369 ± 0.801	2.48	3.60	0.84	0.0060	2.53	13.45	1.167	121
0.175	1.208 ± 0.494	2.41	3.67	0.85	0.0060	2.39	13.04	1.159	146
0.223	1.405 ± 0.435	2.34	3.77	0.86	0.0077	2.27	12.29	1.212	127
0.274	0.856 ± 0.390	2.24	3.87	0.87	0.0073	2.10	11.51	1.195	120
0.322	0.576 ± 0.293	2.22	3.90	0.87	0.0080	2.07	11.35	1.165	88
0.427	0.012 ± 0.312	2.18	3.93	0.88	0.0087	2.00	11.10	1.212	62
0.475	0.019 ± 0.247	2.23	3.88	0.87	0.0099	2.07	11.51	1.247	44
0.525	0.410 ± 0.217	2.19	3.93	0.88	0.0113	2.02	11.11	1.223	47
0.574	0.300 ± 0.177	2.18	3.96	0.88	0.0103	1.99	10.93	1.221	38
0.621	0.222 ± 0.142	2.19	3.94	0.88	0.0109	2.00	11.07	1.223	33
0.669	0.247 ± 0.167	2.13	4.03	0.88	0.0102	1.91	10.40	1.186	31
0.723	0.114 ± 0.117	2.13	3.99	0.88	0.0083	1.93	10.64	1.173	23
0.777	0.425 ± 0.160	2.14	3.99	0.88	0.0083	1.94	10.66	1.135	38
0.827	0.337 ± 0.164	2.15	3.96	0.88	0.0098	1.96	10.85	1.180	32
0.876	0.211 ± 0.144	2.15	3.96	0.88	0.0107	1.95	10.86	1.238	22
0.923	0.474 ± 0.187	2.13	3.99	0.88	0.0092	1.92	10.59	1.283	20
1.011	0.271 ± 0.228	2.15	3.94	0.88	0.0089	1.96	10.94	1.526	17

section was then corrected by the ratio of the "unradiated" to radiated cross section and the calculation repeated. The method converged to within 1% by the second iteration. The calculation included kinematic effects due to a lower virtual-photon energy and a higher cross section from events that radiated. For the purposes of this calculation, it was assumed that the structure function is independent of W and Q^2. Data reported here and earlier show this to be a reasonably valid assumption.[5,9]

The systematic uncertainty in this method is estimated to be less than 3%, which is a result of the assumption of scaling of the structure function. The omission of hadron radiation terms systematically lowers the radiative correction. It is estimated that the effect of the hadron radiation is less than 10% by comparing the correction using this method to the method of Bartl and Urban[14] for the reaction $\gamma_v p \to \pi^+ n$. The x' dependence of the hadron radiation terms is unknown.

The radiative correction for $p_T^2 < 0.02$ GeV^2 is shown as a function of x', W, and Q^2 in Fig. 4. The shape of the correction is the same over the

W and Q^2 range of the experiment and varies by at most 15% between the two extreme points. For the most part, the difference between data points is less than 10%. This difference is about the same size as the systematic uncertainty in the correction and the statistical uncertainty in the data. For this reason, the radiative corrections have not been included in most of the figures. They are included in the tables, however. The uncorrected data can be recovered by dividing the structure function by the radiative correction.

VI. RESULTS

A. Structure function

To study the scaling of the data we present the structure function as a function of x'. Feynman scaling predicts a shape invariance of the structure function as W and Q^2 are varied, while the more general Bjorken scaling predicts a universal ω dependence. Since the hadron spectrometer was oriented along the virtual-photon direction, most of the data is concentrated around small values of

TABLE IV. The π^- neutron structure function for $p_T^2 < 0.02$ GeV^2 as a function of x' for various W and Q^2. σ_{tot} is the proton virtual-photoproduction total cross section.

x'	F (GeV^{-2})	W (GeV)	Q^2 (GeV^2)	ϵ	p_T^2 (GeV^2)	ω	σ_{tot} (μb)	Rad corr	N
			(a) Data point 8: $W=2.2$ GeV, $Q^2=1.2$ GeV^2						
0.082	0.422 ± 0.414	2.71	0.99	0.87	0.0060	7.76	45.18	1.094	81
0.127	1.027 ± 0.234	2.59	1.03	0.89	0.0074	6.87	45.31	1.114	218
0.175	0.774 ± 0.162	2.44	1.09	0.91	0.0069	5.86	45.65	1.107	267
0.224	0.996 ± 0.151	2.34	1.12	0.92	0.0070	5.27	46.10	1.155	319
0.276	0.554 ± 0.122	2.23	1.15	0.94	0.0065	4.70	46.53	1.179	250
0.324	0.555 ± 0.100	2.18	1.18	0.94	0.0073	4.44	46.76	1.134	267
0.376	0.411 ± 0.091	2.14	1.19	0.94	0.0072	4.21	47.07	1.179	236
0.425	0.490 ± 0.078	2.13	1.19	0.94	0.0089	4.17	47.11	1.174	239
0.474	0.358 ± 0.063	2.20	1.16	0.94	0.0096	4.48	46.75	1.198	231
0.525	0.284 ± 0.052	2.19	1.16	0.94	0.0100	4.44	46.58	1.172	238
0.575	0.292 ± 0.051	2.18	1.18	0.94	0.0088	4.35	46.43	1.175	268
0.624	0.215 ± 0.045	2.18	1.18	0.94	0.0081	4.30	46.43	1.184	249
0.675	0.229 ± 0.044	2.15	1.19	0.95	0.0083	4.19	46.58	1.151	309
0.725	0.219 ± 0.043	2.15	1.18	0.95	0.0084	4.19	46.75	1.137	320
0.776	0.308 ± 0.049	2.13	1.19	0.95	0.0085	4.12	46.86	1.100	409
0.824	0.279 ± 0.058	2.14	1.19	0.95	0.0086	4.16	46.76	1.182	458
0.872	0.180 ± 0.057	2.15	1.18	0.95	0.0082	4.17	46.67	1.300	323
0.923	0.305 ± 0.042	2.14	1.19	0.95	0.0091	4.13	46.69	1.410	195
0.982	1.620 ± 0.100	2.12	1.20	0.95	0.0094	4.02	46.70	1.636	566
1.008	0.866 ± 0.067	2.12	1.18	0.95	0.0083	4.07	47.11	1.636	284
			(b) Data point 9: $W=3.1$ GeV, $Q^2=1.2$ GeV^2						
0.040	2.419 ± 1.198	3.22	1.15	0.78	0.0004	9.58	36.88	0.989	22
0.080	0.779 ± 0.355	3.04	1.21	0.82	0.0012	8.38	36.80	1.025	150
0.127	1.064 ± 0.196	3.02	1.22	0.82	0.0029	8.33	36.75	1.040	345
0.176	0.656 ± 0.121	3.00	1.23	0.83	0.0043	8.04	36.58	1.025	437
0.225	0.731 ± 0.102	3.04	1.22	0.82	0.0062	8.30	36.60	1.089	522
0.274	0.603 ± 0.091	3.05	1.21	0.82	0.0073	8.30	36.64	1.130	515
0.324	0.430 ± 0.074	3.06	1.21	0.82	0.0077	8.25	36.48	1.063	425
0.374	0.283 ± 0.068	3.06	1.21	0.82	0.0087	8.22	36.46	1.128	324
0.423	0.264 ± 0.064	3.06	1.21	0.82	0.0101	8.20	36.52	1.108	270
0.476	0.204 ± 0.057	3.10	1.19	0.81	0.0110	8.51	36.63	1.148	241
0.525	0.230 ± 0.044	3.15	1.16	0.80	0.0106	8.96	36.90	1.104	269
0.575	0.248 ± 0.037	3.14	1.17	0.81	0.0093	8.76	36.67	1.104	292
0.625	0.230 ± 0.035	3.12	1.18	0.81	0.0093	8.59	36.54	1.144	294
0.674	0.175 ± 0.033	3.11	1.18	0.81	0.0093	8.57	36.69	1.089	286
0.725	0.157 ± 0.029	3.12	1.18	0.81	0.0103	8.58	36.54	1.076	257
0.775	0.150 ± 0.028	3.10	1.19	0.82	0.0095	8.45	36.59	1.027	243
0.826	0.178 ± 0.033	3.10	1.19	0.82	0.0093	8.38	36.52	1.118	226
0.876	0.310 ± 0.049	3.08	1.20	0.82	0.0094	8.25	36.48	1.251	263
0.921	0.267 ± 0.061	3.07	1.21	0.82	0.0091	8.16	36.38	1.327	273
0.983	0.606 ± 0.057	3.05	1.22	0.83	0.0094	7.96	36.20	1.553	195
1.003	0.122 ± 0.064	3.06	1.19	0.83	0.0077	8.16	36.75	1.553	40

TABLE IV. (*Continued*)

x'	F (GeV^{-2})	W (GeV)	Q^2 (GeV^2)	ϵ	p_T^2 (GeV^2)	ω	σ_{tot} (μb)	Rad corr	N
			(c) Data point 13: $W=2.2$ GeV, $Q^2=4.0$ GeV^2						
0.079	2.654 ± 1.182	2.52	3.59	0.83	0.0037	2.60	13.60	1.155	62
0.126	2.144 ± 0.614	2.54	3.56	0.83	0.0062	2.61	13.86	1.181	114
0.173	0.851 ± 0.413	2.43	3.67	0.85	0.0071	2.42	13.06	1.166	113
0.225	0.765 ± 0.387	2.35	3.77	0.86	0.0075	2.27	12.32	1.218	102
0.275	0.366 ± 0.308	2.27	3.85	0.87	0.0077	2.15	11.75	1.240	69
0.321	0.775 ± 0.265	2.22	3.90	0.87	0.0078	2.07	11.36	1.175	69
0.371	0.082 ± 0.333	2.13	3.99	0.88	0.0099	1.95	10.54	1.228	37
0.425	0.701 ± 0.229	2.17	3.95	0.88	0.0107	2.00	10.92	1.223	48
0.476	0.250 ± 0.200	2.16	3.95	0.88	0.0096	1.98	10.94	1.253	39
0.525	0.244 ± 0.151	2.25	3.84	0.87	0.0112	2.10	11.82	1.226	43
0.572	0.146 ± 0.146	2.15	4.00	0.88	0.0082	1.95	10.65	1.226	39
0.622	0.167 ± 0.121	2.18	3.92	0.88	0.0101	2.00	11.11	1.233	32
0.672	0.070 ± 0.105	2.17	3.96	0.88	0.0090	1.97	10.88	1.197	23
0.769	0.035 ± 0.124	2.14	3.97	0.88	0.0074	1.93	10.69	1.136	17
0.826	0.256 ± 0.098	2.11	4.00	0.89	0.0085	1.90	10.47	1.202	18
0.873	0.326 ± 0.158	2.14	3.95	0.88	0.0074	1.95	10.88	1.316	17
0.925	0.205 ± 0.081	2.10	3.99	0.89	0.0053	1.89	10.49	1.415	7
0.980	0.482 ± 0.174	2.06	4.10	0.89	0.0105	1.82	9.77	1.661	9
1.011	0.566 ± 0.191	2.14	3.95	0.88	0.0107	1.95	10.86	1.661	11

p_T^2. The binning chosen was $p_T^2 < 0.02$ GeV^2, which covers the 360° of azimuth fairly evenly. In Fig. 5 the π^+ and π^- structure functions are displayed as a function of x' for the hydrogen data and in Fig. 6 for the neutron data. The narrow peak at $x'=1.0$ is from the exclusive reactions $\gamma p \to \pi^+ n$ and $\gamma n \to \pi^- p$. The broader peak at $x' \simeq 0.8$ is from the reactions $\gamma p \to \pi^+ \Delta^0$, $\pi^- \Delta^{++}$ and $\gamma n \to \pi^+ \Delta^-$, $\pi^- \Delta^+$. Below x' of 0.8 is the inclusive region. Tables I–IV summarize the structure-function x'-dependence results of this experiment.

The π^+ structure functions from hydrogen are consistently higher than the π^-, yet both distributions have nearly the same shape. On the logarithmic plot, the π^- distributions are much closer to being a straight line while the π^+ distributions are less smooth. The π^+ and π^- data seem to be approaching one another for $x' < 0.2$ in the lower W

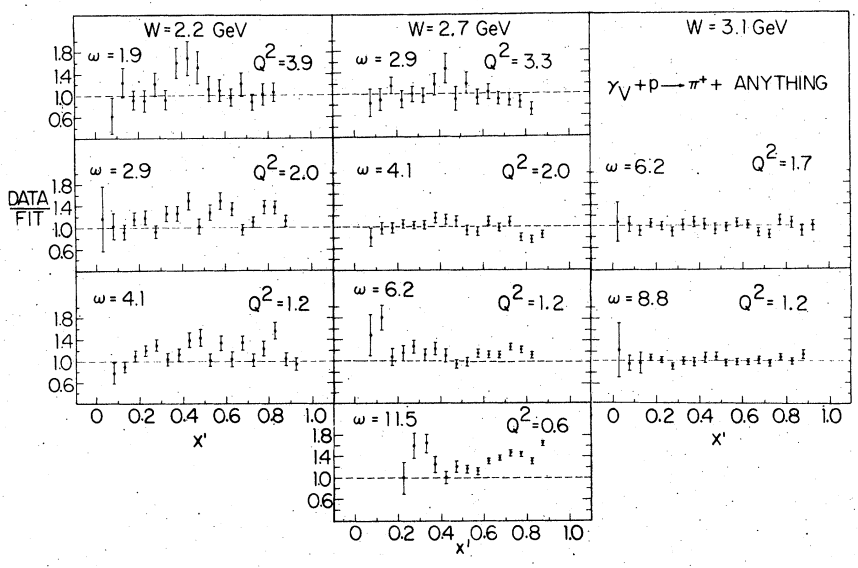

FIG. 7. The π^+ structure functions from the hydrogen target for $p_T^2 < 0.02$ GeV^2 divided by the fit function in Eq. (10).

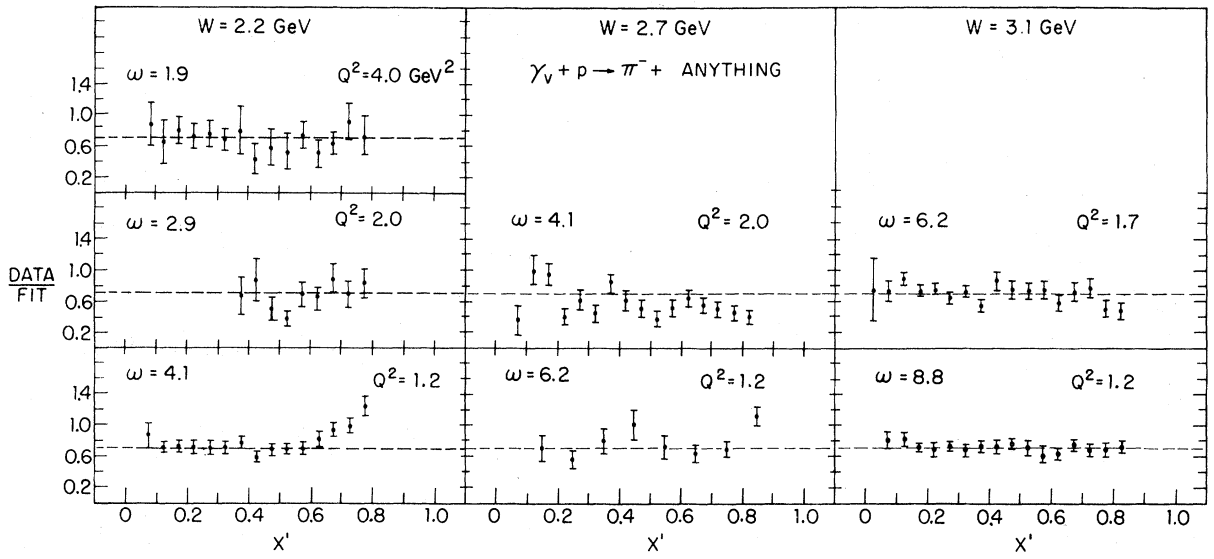

FIG. 8. The π^- structure functions from the hydrogen target for $p_T^2 < 0.02$ GeV^2 divided by the fit function in Eq. (10).

data. Aside from this, the similarity of the data for all data points is the most striking feature. There is little variation with either Q^2 or W. The data from the neutron target is very similar in shape to the proton data and the π^+ and π^- are approximately equal. The statistics of the high-Q^2 neutron data are not very good since they come from a subtraction; it is difficult to draw any conclusions from them. From the above it appears that Feynman x' scaling is a good description of

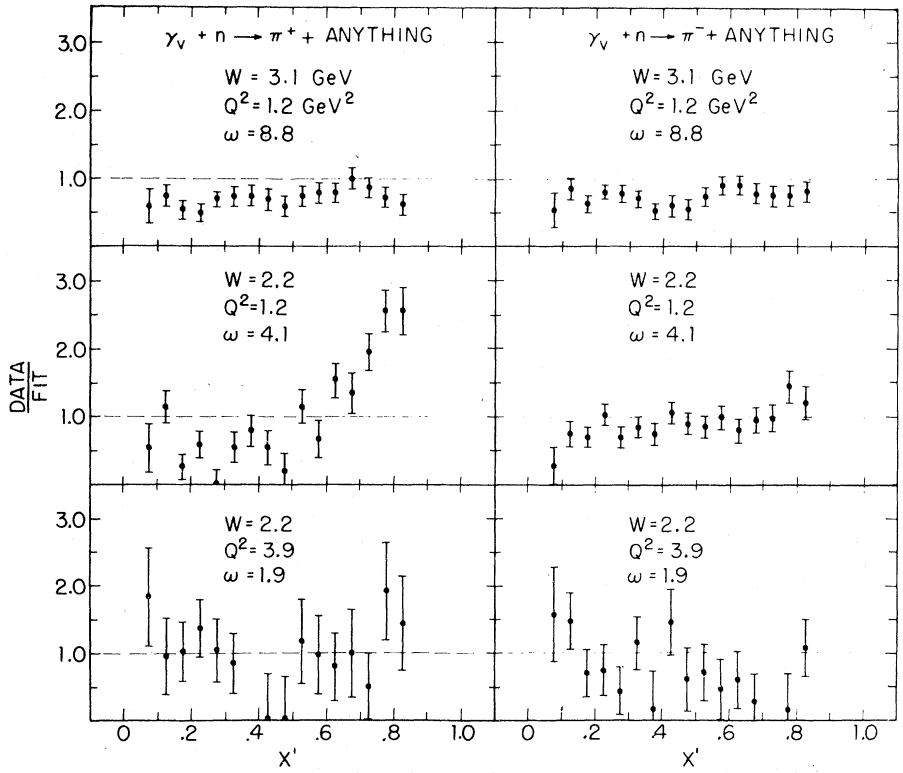

FIG. 9. The π^+ and π^- structure functions from the neutron target for $p_T^2 < 0.02$ GeV^2 divided by the fit function in Eq. (10).

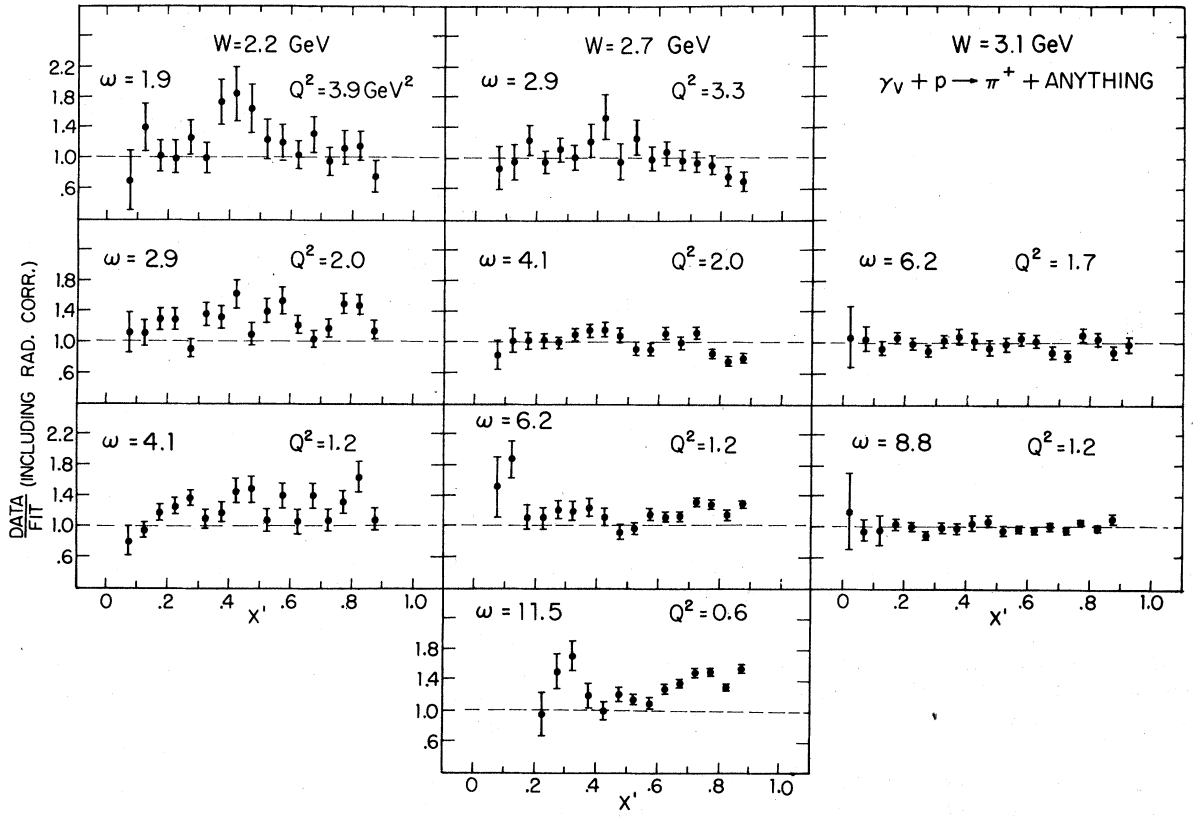

FIG. 10. The radiatively corrected π^+ structure functions from the hydrogen target for $p_T^2 < 0.02$ GeV^2 divided by the fit function in Eq. (11).

the data.

In order to compare the data points more directly the π^+ structure functions at $W = 3.1$ GeV, data points 9 and 10, were fit in the region $0 < x' < 0.8$ and gave the function

$$f = \exp[0.66 - 3.26x' - 3.00(x')^2 + 4.35(x')^3] \ . \quad (10)$$

This function was used only to parameterize the data as a means of comparison. There is no *a priori* reason to believe that the structure function should have this form.

All the structure functions from Figs. 5 and 6 divided by the function f are shown in Figs. 7, 8, and 9. At $W = 2.2$ GeV, the π^+ in Fig. 7 show no substantial change from $Q^2 = 1.2$ to 3.9 GeV^2. There is a broad peak at about $x' = 0.45$ which does not vary with Q^2. This x' value corresponds to a missing mass of about 1.7 GeV. The bump could be due to production of $N^*(1680)$ or $N^*(1700)$ or it could be caused by a difference in the shape of the inclusive spectrum. The effect disappears rapidly with W.

The data at $W = 2.7$ GeV are much flatter and also show little variation with Q^2. The data for $Q^2 \leq 2.0$ GeV^2 are from the earlier experiment[9] but they show no systematic difference from the $Q^2 = 3.3$ GeV^2 data. The broad peak near $x' = 0.7$ in the $Q^2 = 0.6$ GeV^2 data is due to pions from ρ^0 production. The $W = 3.1$ GeV data on the right of Fig. 7 were used to fit the function f and show that the function reproduces the data well.

At fixed Q^2 of 1.2 and 2.0 GeV^2 the data show much more variation with W than with Q^2. As W increases, the data for x' between 0.3 and 0.7 decrease to 1.0 and make the distributions flatter. Data at the same values of ω are diagonally adjacent in Fig. 7. The data at constant ω show this small residual W variation while the data at fixed W are more nearly alike.

The π^- data were divided by the same function, f, and are shown in Fig. 8. The data at $W = 2.2$ GeV are much flatter than the π^+ data and show practically no variation with either Q^2 or W. The rise in the data at $W = 2.2$ GeV, $Q^2 = 1.2$ GeV^2 is caused by a strong $\pi^-\Delta^{++}$ resonance at about $x' = 0.8$. The data seem to be consistent with being flat and a constant fraction, ~0.7, of the function f as shown by the dashed lines in the figure. The neutron data were also divided by the same fit function and are shown in Fig. 9. The π^+ and π^-

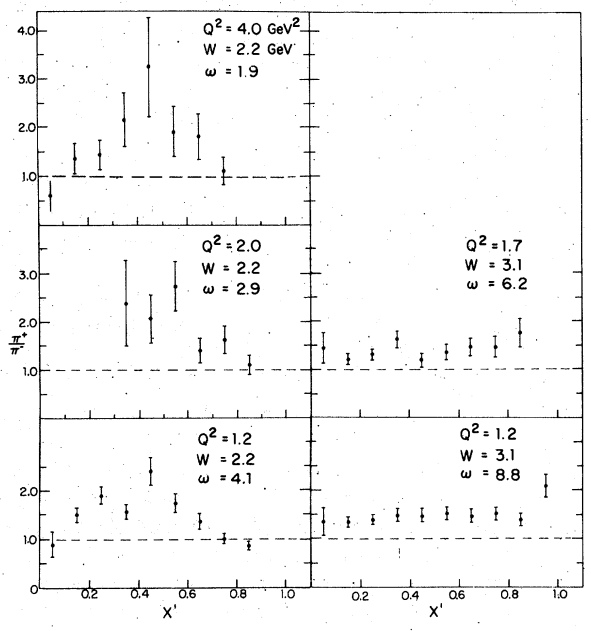

FIG. 11. The π^+/π^- ratio from the proton target as a function of x' for $p_T^2 < 0.02$ GeV^2.

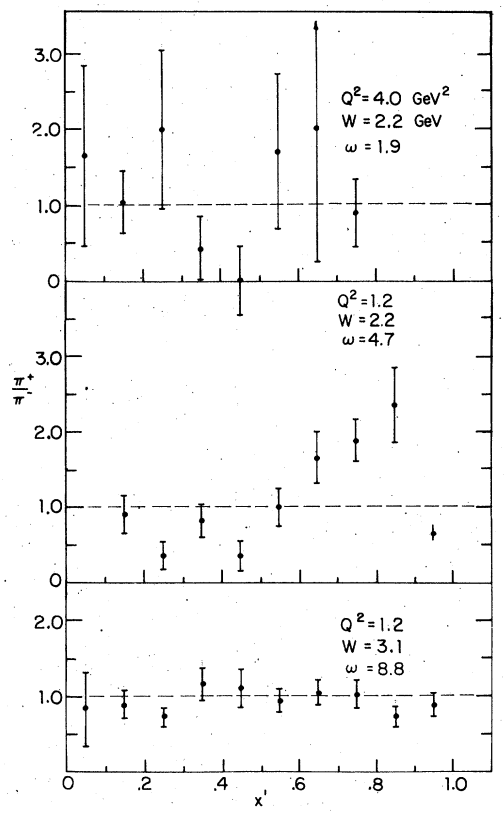

FIG. 12. The π^+/π^- ratio from the neutron target as a function of x' for $p_T^2 < 0.02$ GeV^2,

data are nearly the same. Within the statistics of the data there does not appear to be any systematic variation with W or Q^2.

Figure 10 shows the π^+ hydrogen data including the radiative correction. The function by which the data were divided was

$$g = \exp[0.56 - 1.85x' - 5.98(x')^2 + 6.26(x')^3] \ , \quad (11)$$

determined by refitting the data from points 9 and 10 after the radiative corrections were applied. There is virtually no difference between Figs. 7 and 10. The changes introduced by the radiative correction are small compared to the W dependence and the statistical uncertainties of the data.

B. Charge ratio

The ratio of π^+ to π^- produced in the forward direction is predicted by the quark model to be a universal function of ω.[15,16] The x' dependence of

TABLE V. The pion charge ratio, π^+/π^-, for several x' and p_T^2 regions from proton and neutron targets.

Data point	W (GeV)	Q^2 (GeV^2)	ω	$p_T^2 < 0.02$ GeV^2 $0.1 < x' < 0.4$	$0.4 < x' < 0.7$	$0.7 < x' < 0.9$	$p_T^2 < 0.2$ GeV^2 $0.3 < x' < 0.7$
				(a) Proton target			
8	2.2	1.2	4.1	1.70 ± 0.10	1.79 ± 0.12	0.92 ± 0.07	1.62 ± 0.05
12	2.2	2.0	2.9	2.90 ± 1.10	1.91 ± 0.22	1.35 ± 0.17	1.87 ± 0.12
13	2.2	4.0	1.9	1.53 ± 0.21	2.10 ± 0.34	1.50 ± 0.32	1.85 ± 0.15
9	3.1	1.2	8.3	1.38 ± 0.07	1.43 ± 0.08	1.45 ± 0.10	1.49 ± 0.05
10	3.1	1.7	6.2	1.35 ± 0.08	1.27 ± 0.09	1.60 ± 0.18	1.48 ± 0.06
				(b) Neutron target			
8	2.2	1.2	4.1	0.60 ± 0.12	0.97 ± 0.15	2.00 ± 0.25	0.96 ± 0.08
13	2.2	4.0	1.9	1.13 ± 0.31	1.31 ± 0.45	2.50 ± 1.60	1.33 ± 0.22
9	3.1	1.2	8.3	0.89 ± 0.10	1.11 ± 0.11	0.91 ± 0.12	1.02 ± 0.07

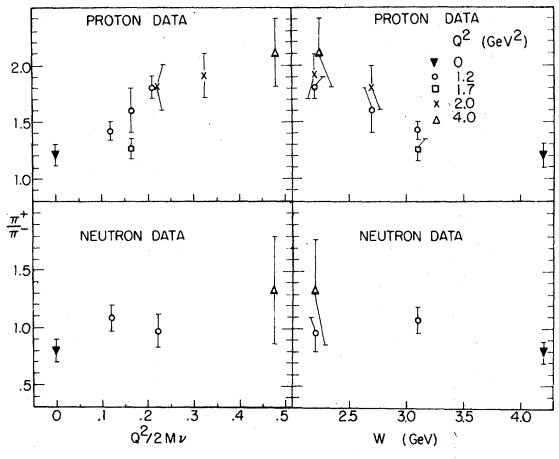

FIG. 13. The π^+/π^- ratio for $p_T{}^2 < 0.02$ GeV^2 and $0.4 < x' < 0.7$ as a function of W and $1/\omega$. The photoproduction data are from Ref. 18.

the ratio depends on what one assumes for the parton fragmentation functions. A decrease in the ratio for increasing W is predicted by thermodynamic models.[17] In Fig. 11 is shown the π^+/π^- ratio from hydrogen for $p_T{}^2 < 0.02$ GeV^2 as a function of x' for each data point. The ratios at the lower W show a broad peak around $x = 0.5$ but become x' independent at $W = 3.1$ GeV. For x' below 0.2 and above 0.6, the ratio at $W = 2.2$ GeV is depressed below the level of the flat distribution at the higher W. This is a reflection of the flatness of the π^- data in Fig. 8 and the broad peak in the π^+ data Fig. 7. There is no apparent Q^2 dependence.

The π^+/π^- ratio from the neutron target is shown in Fig. 12 for $p_T{}^2 < 0.02$ GeV^2. Despite the large errors, it is consistent with being flat in the region below $x' = 0.7$. Table V summarizes the results from protons and neutrons for several x' regions.

The π^+/π^- ratio for the x' region $0.4 < x' < 0.7$ is displayed in Fig. 13 as a function of $1/\omega$ and W. Included in the figure are photoproduction results which are seen to be consistent with the electroproduction data.[18] The ratio from the proton target decreases with increasing W and has little Q^2 dependence. Because of the limited range in Q^2 at fixed W and the statistical errors of the ratio, one cannot distinguish between a universal W de-

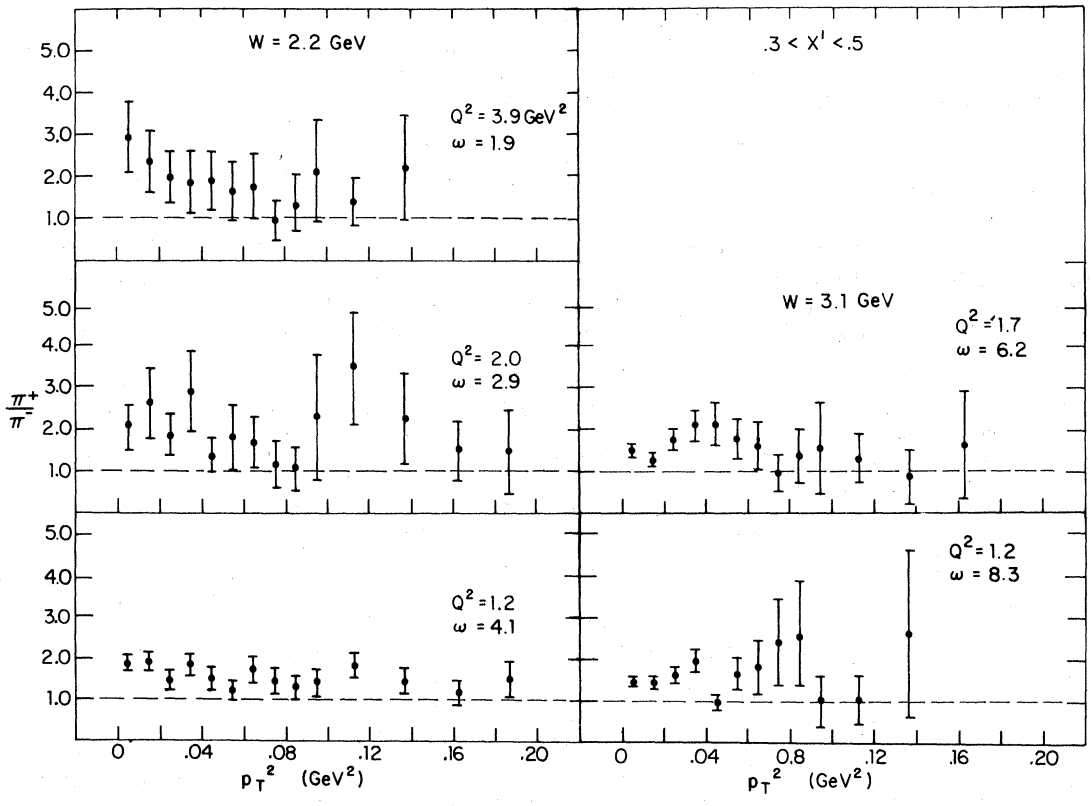

FIG. 14. The π^+/π^- ratio from the proton target as a function of $p_T{}^2$ for $0.3 < x' < 0.5$.

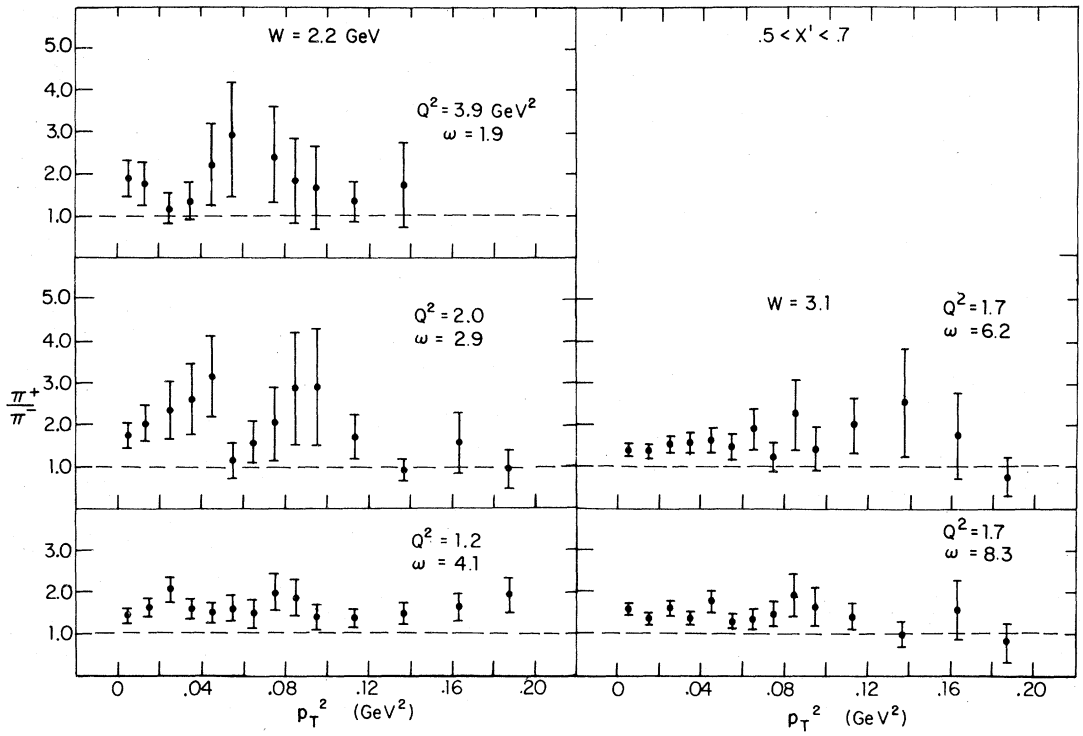

FIG. 15. The π^+/π^- ratio from the proton target as a function of p_T^2 for $0.5 < x' < 0.7$.

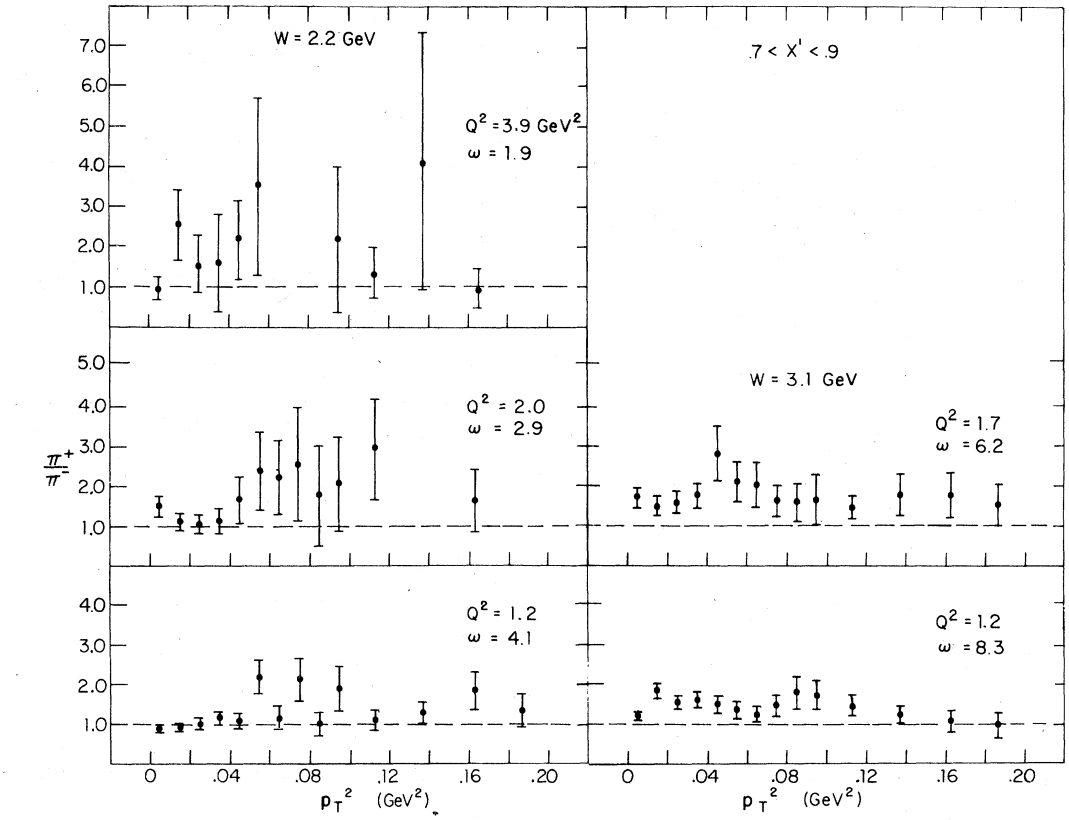

FIG. 16. The π^+/π^- ratio from the proton target as a function of p_T^2 for $0.7 < x' < 0.9$.

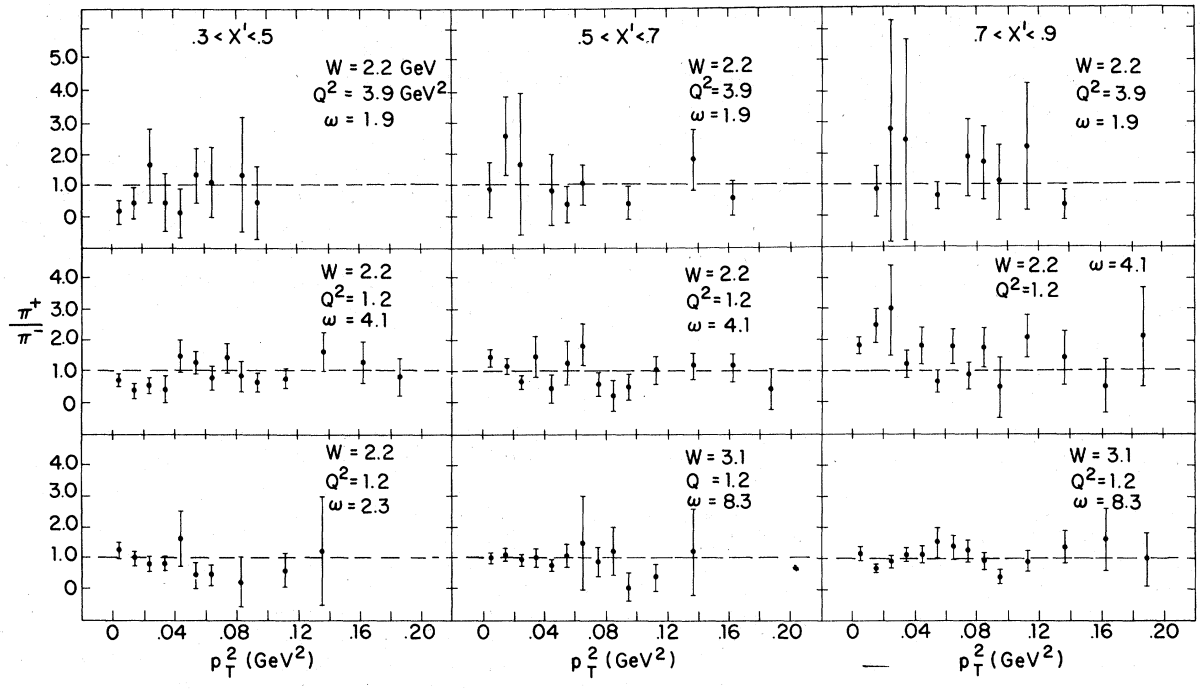

FIG. 17. The π^+/π^- ratio from the neutron target as a function of p_T^2 and x'.

pendence and a universal $1/\omega$ dependence. The data from the neutron target may also show a small drop in the ratio with increasing W, but they are also consistent with having a constant value of 1 independent W, Q^2, and ω.

The p_T^2 dependence of the π^+/π^- ratio is shown for the three x' regions in Figs. 14, 15, and 16 for the proton data and in Fig. 17 for the neutron data. There are no strong variations with either p_T^2 or x'. The data at the lower W may well have

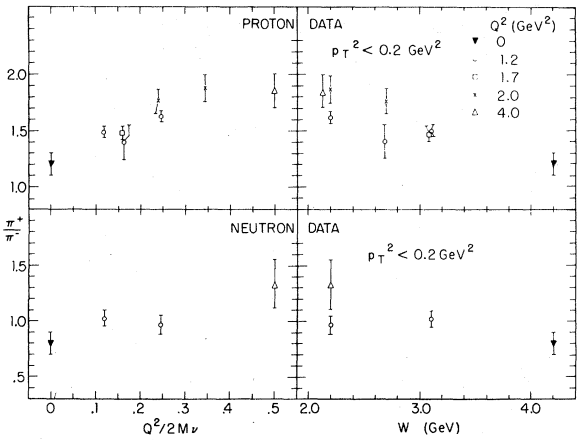

FIG. 18. The π^+/π^- ratio for $p_T^2 < 0.20$ GeV^2 and $0.3 < x' < 0.7$ as a function of W and $1/\omega$. The photoproduction data are from Ref. 18.

a small drop in the ratio with increasing p_T^2, although they are also consistent with being independent of p_T^2. This general p_T independence of the π^+/π^- ratio implies similar p_T dependences for the π^+ and π^- structure functions.

Since there are no dramatic changes in the π^+/π^- ratio with p_T^2, we have formed the ratio for $p_T^2 < 0.20$ GeV^2 and $0.3 < x' < 0.7$ to obtain better statistics. This is shown in Fig. 18 as a function of W and $1/\omega$ and in the last column of Table V. With the enhanced statistics even less Q^2 variation is seen in the data, but on the basis of these data an unambiguous distinction still cannot be made between a universal W or ω dependence, which are of course mutually exclusive. Combination of these data and data obtained in a subsequent experiment[19] indicate a universal ω dependence.

VII. CONCLUSIONS

The parton model predicts a scaling behavior in the variable ω. At the 30% level, the data are ω-independent and scale in the trivial sense; the data do not vary with W, Q^2, or ω. At a finer level, differences of about 10–20% are seen in the π^+ hydrogen data between points at the same ω and different W. The data at fixed W show virtually no change with Q^2. At fixed Q^2 they show a weak W dependence.

The π^- hydrogen data show less variation than

the π^+ data. The π^- data do not change with either W, Q^2, or ω. The neutron data also appear to show scaling in the trivial sense. Any small W or Q^2 variations are masked by the limited statistics.

The pion charge ratios show a systematic decrease with W and little or no Q^2 dependence. Parton models predict that the π^+/π^- ratio should be a function of ω only. Although our results are consistent with a universal ω dependence, the individual structure functions favor a W dependence rather than a universal ω dependence. Data of greater precision and spanning a larger Q^2 range at fixed W or fixed ω will be needed to resolve this ambiguity.

ACKNOWLEDGMENTS

We wish to acknowledge the support of Professor Boyce McDaniel, the staff of the Wilson Synchrotron Laboratory, and the staff of the Harvard High Energy Physics Laboratory. We would like to thank the Electron Scattering Group at Cornell for the use of their spectrometer.

---

*Work supported in part by the U. S. Energy Research and Development Administration under Contract No. AT(11-1)-3064.

†Present address: Fermi National Accelerator Laboratory, P. O. Box 500, Batavia, Illinois 60510.

‡Present address: Laboratory of Nuclear Studies, Cornell University, Ithaca, New York 14853.

§Present address: Nevis Laboratory, Columbia University, Irvington-on-Hudson, New York 10533.

||Present address: P. O. Box 29246, Los Angeles, California 90029.

¶Present address: 36 Webb St., Lexington, Massachusetts 02173.

[1]J. I. Friedman and H. W. Kendall, Ann. Rev. Nucl. Sci. 22, 203 (1972).

[2]R. P. Feynman, in *High Energy Collisions*, edited by C. N. Yang *et al.* (Gordon and Breach, New York, 1969), p. 237.

[3]M. Gell-Mann, Phys. Lett. 8, 214 (1964); G. Zweig, CERN Report No. TH401, 1964 (unpublished).

[4]R. P. Feynman, *Photon Hadron Interactions* (Benjamin, Reading, Mass., 1972).

[5]C. J. Bebek, C. N. Brown, M. Herzlinger, S. D. Holmes, C. A. Lichtenstein, F. M. Pipkin, S. Raither, and L. K. Sisterson, Phys. Rev. Lett. 34, 759 (1975).

[6]L. N. Hand, Phys. Rev. 129, 1834 (1963).

[7]W. B. Atwood, private communication.

[8]Significant deviation of the neutron total cross section from this simple form occurs for $1/\omega > 0.8$, which is beyond the region of this experiment.

[9]C. J. Bebek, C. N. Brown, M. Herzlinger, C. A. Lichtenstein, F. M. Pipkin, L. K. Sisterson, D. Andrews, K. Berkelman, D. G. Cassel, and D. L. Hartill, Nucl. Phys. B75, 20 (1974).

[10]L. Hulthén and M. Sugawara, in *Handbuch der Physik*, Vol. XXXIX, edited by S. Flügge (Springer, Berlin, 1957).

[11]F. Brasse, in *Proceedings of the Sixth International Symposium on Electron and Photon Interactions at High Energy*, Bonn, Germany, 1973, edited by H. Rollnik and W. Pfeil (North-Holland, Amsterdam, 1974).

[12]R. J. Glauber, Phys. Rev. 100, 242 (1955); V. Franco and R. J. Glauber, *ibid.* 142, 1195 (1966).

[13]L. W. Mo and Y. S. Tsai, Rev. Mod. Phys. 41, 205 (1969).

[14]A. Bartl and P. Urban, Acta Phys. Austriaca 24, 139 (1966).

[15]J. Cleymans and R. Rodenberg, Phys. Rev. D 9, 155 (1974).

[16]J. T. Dakin and G. J. Feldman, Phys. Rev. D 8, 2862 (1973).

[17]R. Hagedorn, Nucl. Phys. B24, 93 (1970).

[18]J. Gandsman, G. Alexander, S. Dagan, L. D. Jacobs, A. Levy, D. Lissauer, and L. M. Rosenstein, Nucl. Phys. B61, 32 (1973).

[19]C. J. Bebek, A. Browman, C. N. Brown, K. M. Hanson, S. D. Holmes, R. V. Kline, D. Larson, F. M. Pipkin, S. W. Raither, A. Silverman, and L. K. Sisterson, Phys. Rev. Lett. 37, 1320 (1976).